Genetics: Early Online, published on March 3, 2017 as 10.1534/genetics.117.200238

Annealing of complementary DNA sequences during double-strand break repair in *Drosophila* is mediated by the ortholog of SMARCAL1

Julie Korda Holsclaw* **and Jeff Sekelsky*,†,‡,1**

*Curriculum in Genetics and Molecular Biology, †Department of Biology, ‡Integrative Program in Biological and Genome Sciences, University of North Carolina, Chapel Hill, North Carolina 27599

ABSTRACT DNA double-strand breaks (DSBs) pose a serious threat to genomic integrity. If unrepaired, they can lead to chromosome fragmentation and cell death. If repaired incorrectly, they can cause mutations and chromosome rearrangements. DSBs are repaired using end-joining or homology-directed repair strategies, with the predominant form of homology-directed repair being synthesis-dependent strand annealing (SDSA). SDSA is the first defense against genomic rearrangements and information loss during DSB repair, making it a vital component of cell health and an attractive target for chemotherapeutic development. SDSA has also been proposed to be the primary mechanism for integration of large insertions during genome editing with CRISPR/Cas9. Despite the central role for SDSA in genome stability, little is known about the defining step: annealing. We hypothesized that annealing during SDSA is performed by the annealing helicase SMARCAL1, which can anneal RPA-coated single DNA strands during replication-associated DNA damage repair. We utilized unique genetic tools in *Drosophila melanogaster* to test whether the fly ortholog of SMARCAL1, Marcal1, mediates annealing during SDSA. Repair that requires annealing is significantly reduced in *Marcal1* null mutants in both a synthesis-dependent and synthesis-independent (single-strand annealing) assays. Elimination of the ATP binding activity of Marcal1 also reduced annealing-dependent repair, suggesting that the annealing activity requires translocation along DNA. Unlike the null mutant, however, the ATP binding-defect mutant showed reduced end-joining, shedding light on the interaction between SDSA and end-joining pathways.

KEYWORDS SDSA; DSB repair; SMARCAL1; *Drosophila*; homologous recombination

Introduction

DNA double-strand breaks (DSBs) are deleterious to viability in somatic cells. DSBs can arise from exogenous sources such as chemical mutagens in the environment and ionizing radiation (Ciccia and Elledge 2010; Sage and Shikazono 2016). They can also occur as a byproduct of endogenous processes including replication errors, cellular metabolism resulting in oxidative stress, and repair of other types of lesions that are converted into a DSB for processing (Pfeiffer *et al.* 2000). Unrepaired DSBs lead to chromosome fragmentation and apoptosis; aberrant repair can cause insertions or deletions, as well as chromosomal rearrangements through inappropriate recombination (Tsai and Lieber 2010). It is vital that DSBs are not only repaired, but repaired in such a way as to restore the integrity of the genome.

There are multiple strategies for repairing DSBs that can be separated into two main categories: strategies that do not require a template for repair, which include multiple forms of end joining (EJ); and strategies that do require a template, which are classified as homology-directed repair (HDR; Figure 1). EJ via direct ligation or with minor processing of the ends can be employed immediately at the break, as is the case with canonical non-homologous end joining (cNHEJ; Figure 1G) (Mimitou and Symington 2009; Waters *et al.* 2014; Williams *et al.* 2014). EJ can also be used as an exit strategy after resection via microhomology-mediated end joining (MMEJ). In metazoans, this process requires DNA polymerase theta, and has recently

doi: 10.1534/genetics.XXX.XXXXXX
Manuscript compiled: Wednesday 1st March, 2017%
[1]Corresponding Author: 303 Fordham Hall, Department of Biology, University of North Carolina, Chapel Hill, NC 27599-3280. E-mail: sekelsky@unc.edu

been called theta-mediated end joining (TMEJ; 1H-I) (Chan *et al.* 2010; Yu and McVey 2010; Garcia *et al.* 2011; Yousefzadeh *et al.* 2014; Rodgers and McVey 2016; van Schendel *et al.* 2016; Wyatt *et al.* 2016).

HDR strategies for repair share a common set of steps that begins with resection of the 5′ ends of the break to yield 3′ single-stranded DNA tails that are protected by the single-strand binding protein RPA (Figure 1B). Studies in yeast and *Drosophila melanogaster* have shown that it is possible for complementary resected ends to anneal to each other in a process called single-strand annealing (SSA) (Figure 1J-K), and SSA has been hypothesized to occur in regions of direct repeats (Rong and Golic 2003; Storici *et al.* 2006; Bhargava *et al.* 2016). In non-repetitive regions, Brca2 and other proteins facilitate exchange of RPA for Rad51 on the resected tails, creating a filament competent to search for and invade a homologous duplex template, typically the sister chromatid or homologous chromosome (Jensen *et al.* 2010; Reuter *et al.* 2014). The invading strand anneals to the template strand, displacing its complement and generating a structure called a D-loop (Figure 1C). The invading strand is then extended by synthesis, using the homologous sequence as a template.

It is at this point that the HDR strategies diverge. In synthesis-dependent strand annealing (SDSA) (central model in Figure 1), the D-loop is disassembled and a complementarity test between the nascent strand and the opposing end of the break is performed (1D). If complementarity is found, the two ends anneal. Trimming of non-complementary overhangs, filling of gaps, and ligation restore a duplex DNA molecule (1E-F) (Gloor *et al.* 1991; Nassif and Engels 1993; Pâques *et al.* 1998). An alternative form of HDR occurs when the opposing end of the break anneals to the D-loop in a process called 2nd-end capture (Figure 1L). Continued synthesis from both ends and subsequent ligation produces a joint molecule called a double Holliday junction (dHJ) (Figure 1M), which must be further processed to give duplex products (Figure 1N-Q).

HDR leading to dHJ formation is often invoked as a primary form of templated repair in somatic cells, though this interpretation is largely due to studies of meiotic recombination mechanisms (reviewed in Jasin and Rothstein 2013). During meiotic recombination, the dHJ pathway is important because it can generate the crossovers that are necessary for homolog disjunction; however, crossovers can be detrimental to mitotically proliferating cells. It is thought that crossovers are avoided in somatic cells either through biased processing of dHJs or by disfavoring formation of dHJ intermediates (Ira *et al.* 2003; Andersen *et al.* 2011; Kuo *et al.* 2014; Sarbajna *et al.* 2014; LaFave *et al.* 2014). SDSA is gaining acceptance as a predominant form of HDR in mitotic cells due to its parsimony and a growing amount of circumstantial evidence, such as the rarity of mitotic crossovers in wild-type backgrounds (reviewed in Andersen and Sekelsky 2010). Despite this growing support, there are few assays in existence with the capacity to determine whether non-crossover gene conversion events were generated through the SDSA or the dHJ pathway. As such, little is known about the defining step of SDSA: annealing.

Annealing is the step at which the cell commits to SDSA (Figure 1D), so understanding this step is critical to understanding DSB repair. Studies in budding yeast have identified Rad52 as an important mediator of annealing during SSA (Ivanov *et al.* 1996; Storici *et al.* 2006; Jensen 2013). Mammalian Rad52 mutations do not result in strong HDR defects (Rijkers *et al.* 1998), although human RAD52 has been found to be important for 2nd-end capture through interactions with RPA and Rad51 (McIlwraith and West 2008; Nimonkar *et al.* 2009; Khade and Sugiyama 2016). This suggests that Rad52 functions in animals may be confined to steps of HDR where Rad51 is active, such as strand invasion, making it unlikely that RAD52 is the mediator of annealing during SDSA.

Recent studies in mammalian systems have uncovered a class of helicases with ATP-driven annealing activity called annealing helicases (Yuan *et al.* 2012). Members of this family can anneal two RPA-coated, complementary single DNA strands, making these enzymes ideal candidates for annealing during SDSA. The first member of this family to be identified, SMARCAL1, has a C-terminal Swi/Snf2 family helicase domain and two N-terminal HARP domains (SMARCAL1 was originally called HARP for HepA-Related Protein) (Coleman *et al.* 2000; Yusufzai and Kadonaga 2008). SMARCAL1 plays roles in replication-associated DNA damage repair and has been shown to regress model replication forks by annealing the parental strands (Bétous *et al.* 2012). SMARCAL1 is activated by ATR-dependent phosphorylation and recruited to troubled forks via an interaction with RPA (Ciccia *et al.* 2009). Biallelic mutations in *SMARCAL1* cause the autosomal recessive disorder Schimke immuno-osseous dysplasia (SIOD). SIOD patients have multiple clinical features, some of which are similar to those of DNA damage repair disorders such as Bloom syndrome and Fanconi anemia. These include poor growth, immune-deficiencies, and premature aging symptoms (Lou *et al.* 2002; Baradaran-Heravi *et al.* 2012b; Morimoto *et al.* 2016).

Orthologs of SMARCAL1 are found throughout metazoans, as well as in plants and some protists, though are notably absent from yeasts. *Drosophila melanogaster* Marcal1 is 41% identical and 60% similar to human SMARCAL1 across the helicase domain (based on BLAST alignment of residues 154-679 of Marcal1 to residues 337-869 of SMARCAL1). Marcal1 has a single HARP domain versus the two in SMARCAL1; the presence of two HARP domains appears to be unique to chordates. The distance between the helicase ATPase domain and the proximal HARP domain is critical for the annealing function of SMARCAL1 *in vitro* (Ghosal *et al.* 2011), and that distance is conserved in Marcal1. *In vitro* studies comparing the activity of Marcal1 to SMARCAL1 showed that both proteins have robust annealing activity (Kassavetis and Kadonaga 2014). Further support for a role of Marcal1 in annealing during SDSA is suggested by a previous study showing that mutations in *mei-41*, which encodes the *Drosophila* ortholog of ATR, significantly reduce annealing during both SDSA and SSA (LaRocque *et al.* 2007), suggesting that an ATR-activated protein, such as SMARCAL1/Marcal1, catalyzes annealing during DSB repair.

Drosophila is one of the few model organisms with genetic tools available to assay SDSA, making it an ideal system to test whether SMARCAL1 plays a role in annealing during SDSA *in vivo*. We show here that *Drosophila Marcal1* mutants have elevated lethality when exposed to DSB-inducing agents, indicating Marcal1 has a role in HDR. We used well-characterized assays to demonstrate that annealing during both SDSA and SSA is severely reduced in *Marcal1* mutants. Abrogating Marcal1 ATP-binding reduces EJ as well as annealing, suggesting that Marcal1 activity is epistatic to TMEJ. Altogether, these data uncover new information about HDR that further our understanding of DSB repair, which will aid in improving the efficiency of chemotherapeutics as well as laboratory technologies such as CRISPR/Cas9.

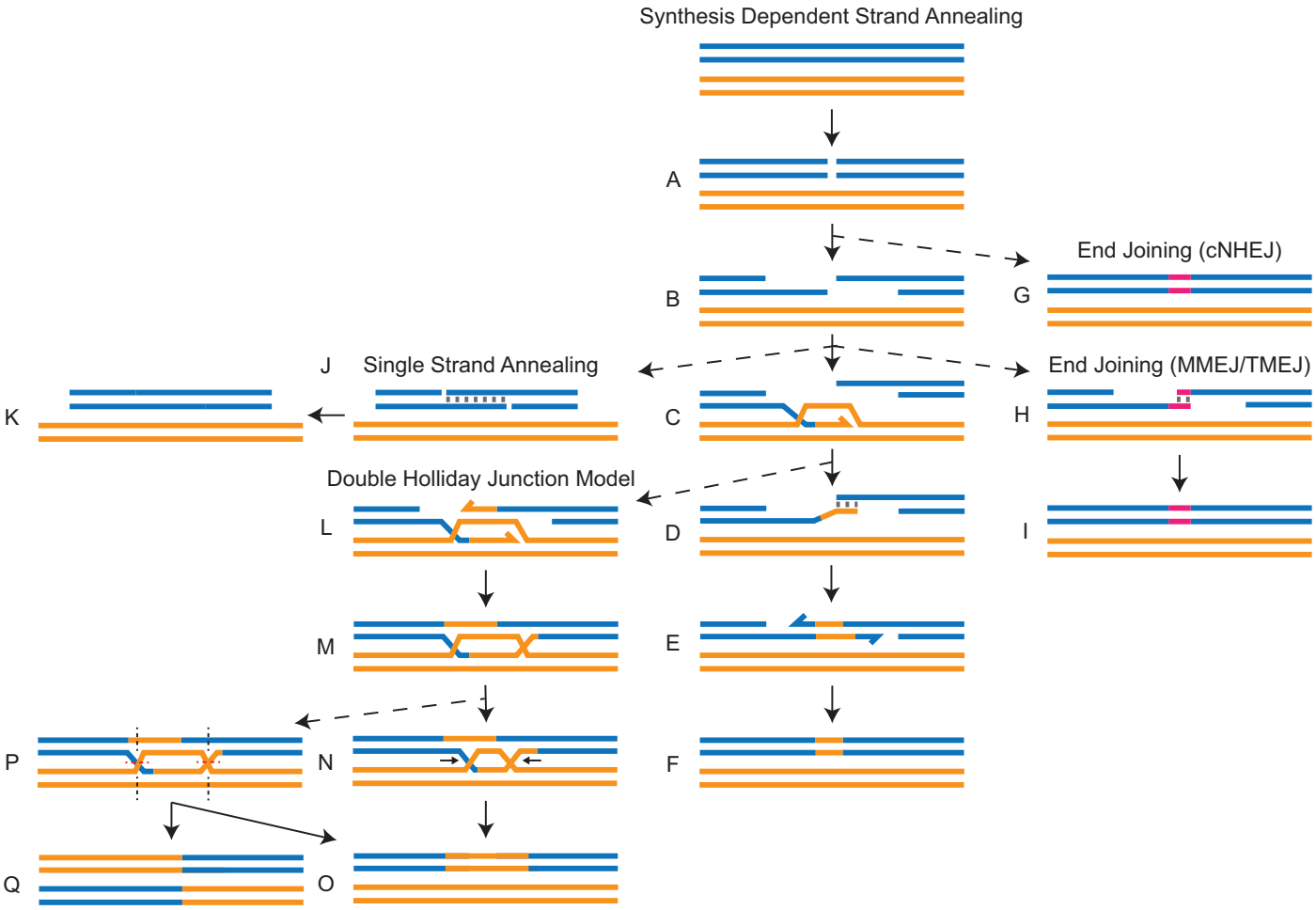

Figure 1 DSB repair strategies. Blue: dsDNA molecule; orange: dsDNA template (sister chromatid or homologous chromosome). (A) A DSB occurs in the blue DNA molecule. (B) 5′ resection marks the first step of homology-directed repair and results in 3′ ssDNA tails. (C) Rad51-coated ssDNA tail invades a template duplex, displacing one strand to creating a D-loop, and primes synthesis. (D) The D-loop is disassembled and a complementarity test between the opposing ends of the break occurs. (E) SDSA is defined by annealing between complementary sequences, followed by trimming and/or gap filling. (F) Ligation restores an intact duplex DNA molecule. Alternative strategies (dotted arrows). (G) Canonical non-homologous end joining can occur instead of resection, which directly ligates the ends and can generate small insertions and deletions (pink segment). (H) Microhomology-mediated end joining (catalyzed by DNA polymerase theta in metazoans) can occur prior to strand exchange or after failure to find or anneal at complementary sequences. (I) MMEJ/TMEJ can will usually generate a deletion or insertion (pink segment). (J) If the DSB occurs between two direct repeats, complementary sequences may be exposed during resection, and annealing can occur without synthesis, called single-strand annealing (SSA). (K) SSA results in deletion of one repeat. (L) 2nd-end capture (annealing of the opposing strand to the D-loop, allowing for extension of that strand) can occur during synthesis. (M) Ligation to the opposing 5′ ends creates a double-Holliday junction (dHJ). (N) Dissolution of the dHJ involves migration of the junctions toward each other and decatenation via topoisomerase activity to (O) restore the DNA molecule. (P) Resolution involves endonucleolytic cleavage of the junctions which can be cut in either orientation, resulting in both (O) non-crossover (restoration of the DNA molecule) and (Q) crossover (recombinant) products.

Materials and Methods

Drosophila stocks

Fly stocks were maintained at 25°on standard cornmeal medium. All *Marcal1 null* assays were performed using heteroallelic null mutations $Marcal1^{del}$ and $Marcal1^{kh1}$. $Marcal1^{del}$ is a 679-bp deletion of part of the first exon and second intron generated via imprecise P-element excision as described in (Baradaran-Heravi *et al.* 2012a). $Marcal1^{kh1}$ was generated using CRISPR/Cas9 technology (Bassett and Liu 2014; Gratz *et al.* 2013). Oligonucleotides (IDT) used for guide RNA were cloned into pU6 *Bbs*I chiRNA vector then injected into Bloomington stock #51323 (y^1M{vas-Cas9}ZH-2Aw^{1118}/FM7c) (BestGene). $Marcal1^{kh1}$ deletes 2L:4,955,554-4,956,729 (*Drosophila* annotated genome r6.13), which encompasses exon 1 through part of exon 2. $Brca2^{43}$ null mutation was used *in trans* to $Brca2^{47}$ null mutation in all assays. Both are large deletions produced via imprecise *P* element excision as described in (Thomas *et al.* 2013).

$Marcal1^{K275M}$ mutation was generated using CRISPR/Cas9. The gRNA vector was prepared as described for the $Marcal1^{kh1}$ allele. A repair template vector was generated by amplifying 1234 bp upstream and 643 bp downstream of the con-

served lysine codon from BacPac genomic DNA clone library (ID BACR13M11) and inserting into the pSL1180 vector. QuickChange Site-Directed Mutagenesis Kit (Agilent Technologies) was used to introduce a mutation in the PAM recognition site as well as two single bp changes to alter the lysine codon to methionine (primer sequence: 5′ GAAATGGGCCTGGGCATGACCTATCAGGCCTTGGC CGTAGCCG-3′). The repair vector was injected with the *Bbs*I chiRNA vector into the same stock used for generating the *Marcal1*^{kh1} allele.

Sensitivity Assays

Vials of five heterozygous *Marcal1*^{del} females and three heterozygous *Marcal1*^{kh1} males each were incubated for three days (brood 1) before being transferred to fresh vials of food for two additional days (brood 2), after which the adult flies were discarded. One day later, 250 ul of aqueous mutagen solution was added directly to the food in brood 2 vials and the larvae were allowed to develop to adulthood (dosages listed in Table S1). For ionizing radiation experiments, larvae were exposed to Cesium-137 for the required time to reach the desired dosage. Surviving adults in both broods were quantified by genotype (heterozygous or heteroallelic null) and the ratio of heterozygous to heteroallelic was calculated per vial. Exposed vials were normalized to unexposed paired brood 1 ratios. Paired *t*-tests were performed between unexposed and exposed ratios. Each round of biological replicates had 10-20 vials and each mutagen had two or more rounds.

P{w^a} Assays

The *P*{*w*^{a}} assay was performed as previously described (Adams *et al.* 2003). Briefly, single males of the genotype *ywP*{*w*^{a}}; *Marcal1*^{del} / *Marcal1*^{kh1}; *Sb P*{Δ 2-3, *ry*$^+$}/*TM6B* were crossed to four females homozygous for *ywP*{*w*^{a}} and *Sb*$^+$ female progeny were scored for red, yellow, or apricot eyes. Representative samples of red and yellow eyed females were collected and crossed to *FM7w* males to recover the repair product in subsequent males. DNA was extracted from a single adult male progeny with the repair product for PCR analysis. Multiple repair events were recovered per male, however, only repair events that could be confirmed unique were analyzed and reported. The same methods and transposase source were used for all genotypes.

Each vial of progeny from a single male was scored independently and a ratio of either red- or yellow-eyed progeny to total progeny was calculated per vial. Outliers were identified using the ROUT method and removed from the data set. No outliers were removed from the *Brca2* data set; one was removed from *Marcal1 Brca2*; and three were removed from *Marcal1*, wild type, and *Marcal1*^{K275M} data sets. To determine and compare mean frequency of repair events, the red-eye (SDSA) ratios were compared between genotypes using parametric ANOVA and the mean ratios of each genotype were compared to the mean ratios of all other genotypes; the analysis was repeated for yellow-eye (EJ) ratios. Rate of lack of excision was calculated by subtracting the EJ rate of *Brca2* mutants from the total scored progeny as *Brca2* mutants are incapable of strand invasion. Rate of complete restoration of *P*{*w*^{a}} was calculated by summing the frequency of all repair events in wild-type males and subtracting that rate from the EJ rate of *Brca2* mutants, using the assumption that all excisions were repaired by EJ in these mutants.

To assess synthesis capability, each repair event was analyzed with a series of seven PCRs (primers are listed in Table S2). Amplified products using one primer set were calculated as a percentage of total events analyzed and repeated for all primer sets (intervals). Percentage of events with positive PCRs were compared between genotypes using parametric ANOVA. When compared as individual PCRs, P <0.05 was considered to be statistically significant; however, when asking how much difference exists between genotypes across all PCRs, P-values for each interval were multiplied by the number of intervals (7) to correct for multiple comparisons.

P{wIw} Assays

The *P*{*wIw*} assay was performed as previously described (Mukherjee *et al.* 2009). Briefly, four *Marcal1*^{del}/*CyO* ; *P*{*wIw*}/*TM6B* females were crossed to three *Marcal1*^{kh1}/*CyO* ; *Sb P*{*70I-SceI*}/*TM6B* males for three days then the parents were discarded. One day later, the 1st-instar larval progeny were heat-shocked at 37^o for one hour. Heat shock was repeated on the following day to ensure all 1st-instar larvae received treatment. Larvae were allowed to develop to adulthood. All *Sb*$^+$ progeny were scored for red or white eyes. All red-eyed flies were collected (up to a maximum of 10) from each vial; 10 white-eyed flies were collected per vial. DNA was extracted from each collected fly for analysis.

Red-eye events: The linker region was amplified (primer sets in Table S3) and subjected to digestion with *I-Sce*I. Events that failed to amplify or were not cut by *I-Sce*I were categorized as EJ events. Events that were successfully cut by *I-Sce*I could not be distinguished between EJ and uncut and were removed from the dataset.

White-eye events: The 5′ region of the upstream mini-white gene is 480 bp whereas the 5′ region of the downstream mini-white is 369 bp using the same primer set (Table S3). The presence of both products indicates SSA did not occur; these events were categorized as EJ events. A small number of events had only the 369-bp product, these were verified to be in the upstream location via primer anchored in the *P* element and categorized as SSA events. PCRs with no product were categorized as EJ events. The percentage of SSA events in the white class was calculated per vial. SSA and EJ events were then adjusted by this number.

The adjusted percentages of SSA events per vial were compared via unpaired *t*-tests between control and mutant genotypes per experiment. *Marcal1*^{K275M} heterozygotes and homozygotes were compared to each other, wild type, and *Marcal1* using parametric ANOVA.

Data Availability

The authors state that all data necessary for confirming the conclusions presented in the article are represented fully within the article. Drosophila stocks are available upon request.

Results

Marcal1 mutants show elevated lethality when exposed to DSB-inducing agents

We tested whether Marcal1 has a role in DSB repair by exposing mutant larvae to DNA damaging agents and measuring survival to adulthood relative to unexposed siblings. *Marcal1* mutant survival was not affected when exposed to methyl methanesulfonate (MMS), an alkylating agent (Lundin *et al.* 2005), or nitrogen mustard (HN2), which generates both mono-adducts and inter-strand crosslinks (Povirk and Shuker 1994) (Figure 2). Studies in mice have shown that *SMARCAL1* null mutations

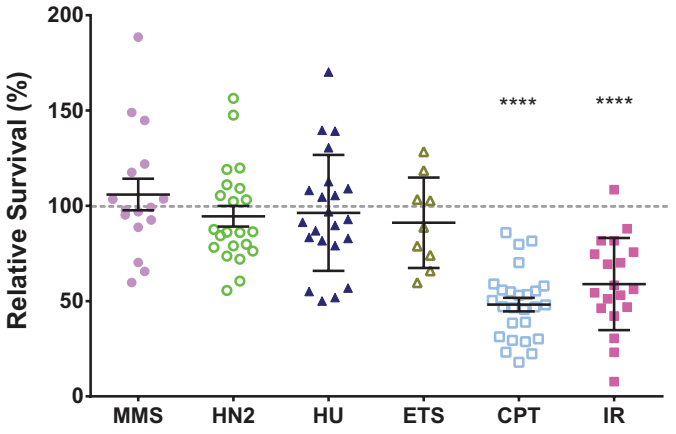

Figure 2 ***Marcal1*** **mutants are sensitive to killing by DSB-inducing agents.** Flies heterozygous for null mutations in *Marcal1* were mated in two broods of at least 10 vials, with each vial representing a biological replicate. Brood one was unexposed; brood two received a dose of MMS (methyl methanesulfonate), HN2 (nitrogen mustard), HU (hydroxyurea), ETS (etoposide), CPT (camptothecin), or IR (ionizing radiation) during larval feeding. Relative survival was calculated as the ratio of homozygous mutant to heterozygous control adults in treated vials, normalized to the same ratio in the corresponding unexposed vial. Dotted line represents 100% relative survival. ****, P <0.0001 in paired t-tests between unexposed and exposed vials. Dosage, number of replicates, and total progeny counts are in Table S1.

confer sensitivity to killing by hydroxyurea (HU) (Baradaran-Heravi *et al.* 2012b), a ribonucleotide reductase inhibitor thought to result in stalled replication forks (Hammond *et al.* 2003); however, *Marcal1* mutant larvae showed no decrease in survival when exposed to HU. HU treatment is most detrimental in cells sensitive to perturbations in replication which is consistent with published *in vitro* evidence that Marcal1 cannot regress a four-stranded model replication fork (Kassavetis and Kadonaga 2014) and suggests Marcal1 may not have a significant role in protecting stalled forks in flies.

We found a significant reduction in survival of *Marcal1* mutant larvae exposed to ionizing radiation (IR), an established DSB-inducing agent (Radford 1985). *Marcal1* mutant flies were also sensitive to killing by camptothecin (CPT), similar to both mouse and human cell studies (Baradaran-Heravi *et al.* 2012b). CPT prevents topoisomerase I from re-ligating DNA after it has nicked a strand and become covalently bound to the end (Pommier *et al.* 2010). CPT is thought to be most lethal during replication, where the nick can become a DSB. Previous studies have suggested that CPT lesions are repaired via HDR in *Drosophila* (Andersen *et al.* 2011) and in chicken DT40 cell lines (Maede *et al.* 2014). Interestingly, *Marcal1* mutant flies did not have elevated lethality when exposed to etoposide (ETS), a topoisomerase II poison that generates DSBs (Pommier *et al.* 2010). A genetic screen of DT40 cells found that mutations in EJ genes conferred sensitivity to ETS and resistance to CPT whereas mutations in HR genes resulted in higher sensitivity to CPT than to ETS (Maede *et al.* 2014). It is possible that *Marcal1* mutants are sensitive to ETS at higher doses than those tested here, however the data from CPT and IR treatments sufficiently support our hypothesis that Marcal1 is involved in DSB repair.

Marcal1 mutants have reduced annealing capacity during gap repair

Because *Marcal1* mutants are sensitive to agents that cause DSBs, we tested the ability of these mutants to repair a double-stranded gap by SDSA. We used the well-characterized $P\{w^a\}$ assay in the germline of male *Drosophila* (Figure 3) (Kurkulos *et al.* 1994; McVey *et al.* 2007). $P\{w^a\}$ is a 14 kb P element that is a non-lethal insertion into the first intron of the essential gene *scalloped* (*sd*) on the X chromosome (Figure 3, inset). The P element contains a *white* (*w*) gene, the product of which loads red pigment into the eye, interrupted by an intronic *copia* retrotransposon flanked by two 276-bp long terminal repeats (LTRs). The *copia* insertion alters *w* splicing and results in an apricot-colored eye in hemizygous males or homozygous females. When exposed to an inefficient source of P element transposase, the $P\{w^a\}$ element is excised from one chromatid; the intact sister chromatid serves as an efficient template for HDR. Excision generates 17-nt non-complementary overhangs on both sides of the break, which are structurally similar to short resected ends and are poor substrates for end-joining via cNHEJ (Symington and Gautier 2011). Repair events from single males are recovered in female progeny by crossing to females homozygous for $P\{w^a\}$.

For SDSA to occur, both sides of the break must be extended (via synthesis) beyond the first region of complementarity, the *copia* LTRs, and these must be annealed correctly (Figure 3). The resultant product deletes *copia* except for a single LTR, resulting in restoration of *w* splicing, observable as red eyes in progeny inheriting this product. If EJ occurs either without synthesis or after incomplete synthesis, *w* function is lost, resulting in yellow-eyed progeny (due to the maternally-inherited complete $P\{w^a\}$ copy). Complete restoration of $P\{w^a\}$ could occur via a dHJ intermediate or through SDSA or EJ that synthesizes past the LTRs. These are not scored as repair events because they cannot be differentiated from a lack of excision; however, lack of excision is the most frequent class (>85% of progeny), whereas complete restoration is estimated to be <2% in wild-type males. SDSA and EJ events are quantified as a percentage of total scorable progeny (daughters that do not inherit the transposase source) from each male, including apricot-eyed progeny. We also measured the distribution of events per male.

We found that *Marcal1* mutants had significantly reduced SDSA (red-eyed progeny) compared to wild type both in percentage of total progeny scored (Figure 4A) and in number of males with observable SDSA events in the progeny (Figure S1). EJ (yellow-eyed progeny) was not significantly changed in Marcal1 mutants (Figure 4B). SDSA could be reduced if P element excision is reduced or strand exchange is impaired. To test this, we performed the assay in a *Brca2* mutant. *Drosophila* Brca2 has a strand exchange function similar to that of human BRCA2 (Brough *et al.* 2008), so we expected strand exchange to be defective in *Brca2* mutants and for all repair to be the result of EJ events prior to strand invasion, which would be observable as yellow-eyed progeny. As expected, we observed no red-eyed progeny in *Brca2* single mutants and a compensatory increase in yellow-eyed progeny compared to wild type (Figure 4A-B). If *Marcal1* mutations reduce P element excision or affect the pathway upstream of Brca2 function in DSB repair, we would expect *Marcal1 Brca2* double mutants to have reduced EJ compared to *Brca2* single mutants due to an overall reduction in observable repair products. However, we found *Marcal1 Brca2* double mutants to have a repair phenotype that was not significantly different from *Brca2* single mutants (Figure 4A and B).

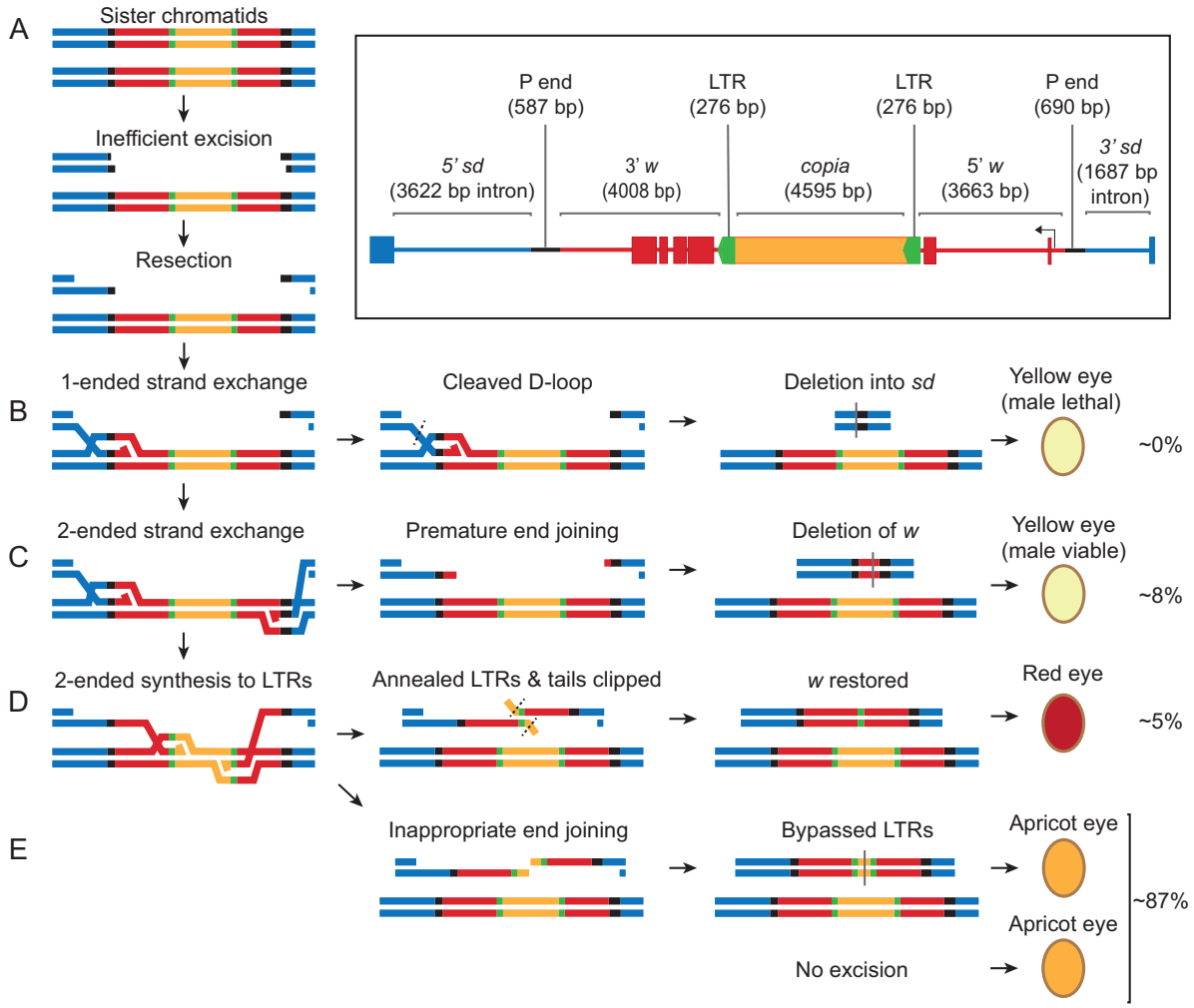

Figure 3 The *P{w^a}* assay for SDSA. *Inset*: The construct is a 14-kb *P* element inserted into the 2nd intron of the essential gene *scalloped* (*sd*) (blue) in reverse orientation (diagram is relative to genome coordinates on *X* chromosome). Black segments represent *P* element sequences needed for excision. Red segments are exons (boxes) and introns (lines) of a *white* (*w*) gene, the product of which loads eye pigments when functional. This copy of *w* is interrupted by a *copia* retrotransposon (orange central box) which is flanked by two 276-bp LTRs (green directional boxes), resulting in partial loss of *w* function and an apricot-eyed phenotype. (A) Line representations of the construct on two sister chromatids in the male germline. Exposure to inefficient P transposase results in excision of the construct from one sister, leaving 17-nt non-complementary overhangs on each side and the ends are resected. (B) One of the 3′ ssDNA tails invades the intact sister to initiate synthesis. If D-loop dissociation is defective, the D-loop is cleaved, creating a deletion into a *sd* exon on one or both sides of the construct. When mated to a homozygous *P{w^a}* female, the progeny with flanking deletions will have a yellow eye (due to the full copy of the construct from the mother) but the event will be male-lethal in subsequent generations (0% of progeny from wild-type males have this phenotype). (C) Premature end joining after two-ended strand exchange and some synthesis results in complete loss of *w* function; progeny will have yellow eyes and viable males in subsequent generations (8% of progeny from wild-type males). (D) Synthesis of the LTRs followed by annealing, tail clipping and gap filling restores *w* function and progeny have a red eye (5% of progeny from wild type males). (E) Synthesis to the LTRs followed by inappropriate end joining in *copia* results in an apricot eye in the progeny and is indistinguishable from non-excision or full gene conversion events via dHJ intermediates (87% of progeny from wild-type males). These progeny are scored but not counted as repair events.

We therefore conclude that the decreased SDSA in *Marcal1* mutants results from a loss of function downstream of strand invasion.

While the *Marcal1* mutant phenotype could result from defective LTR annealing, it could also be due to compromised D-loop disassembly or reduced capacity to synthesize past the LTRs. In *Blm* mutants, which are believed to be defective in D-loop disassembly, the synthesis length in repair products is significantly shorter than in wild-type males (McVey *et al.* 2007). In addition, many repair events have deletions from the break site into the flanking *sd* gene; these are hypothesized to arise from nucleolytic cleavage of D-loops that cannot be disassembled (Adams *et al.* 2003; McVey *et al.* 2004b). We analyzed the aggregated amount of synthesis from each end of the break in all observed EJ events to determine the overall synthesis pattern within the population of EJ events (Figure 4C). Synthesis tracts

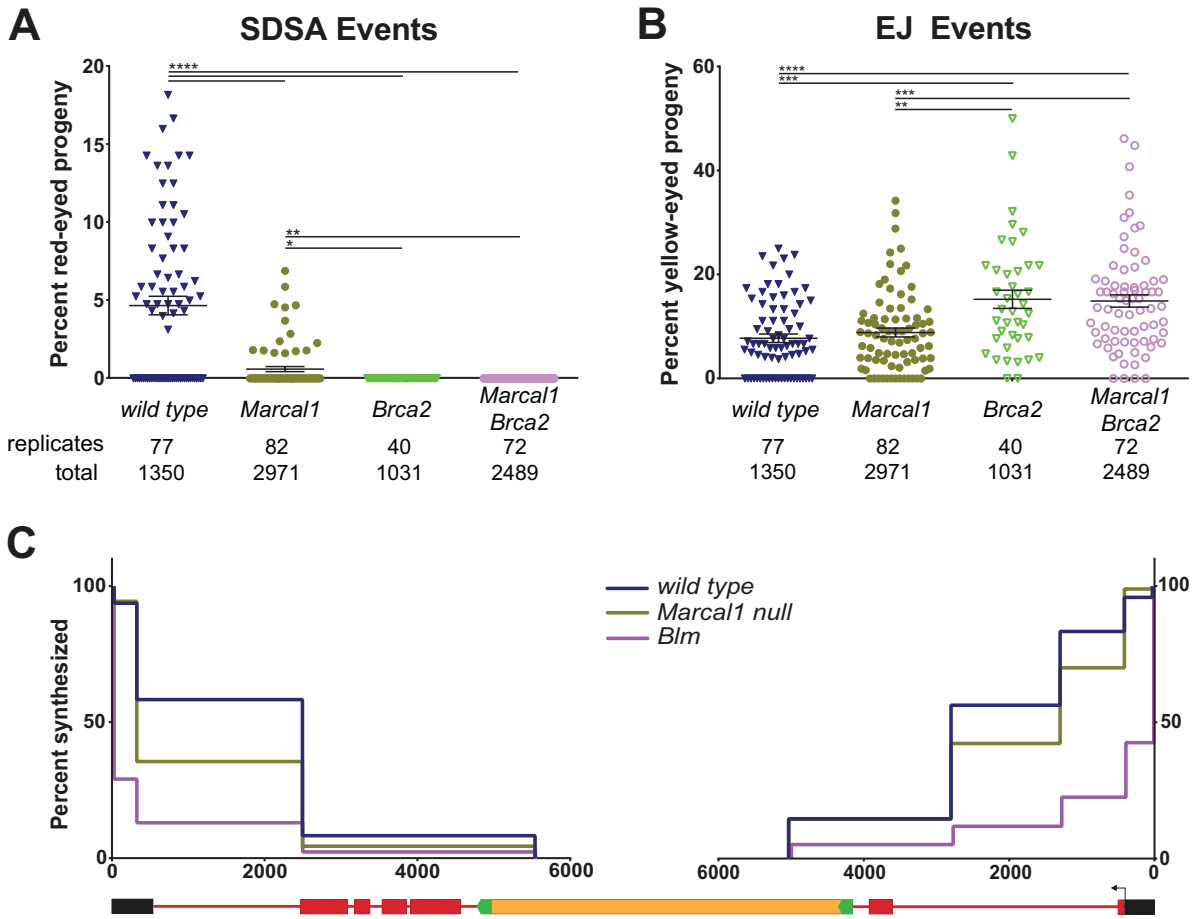

Figure 4 *Marcal1* mutants have reduced SDSA capacity in the $P\{w^a\}$ assay. (A) SDSA events are measured as the percentage of scored progeny with red eyes. Mean and SEM are indicated. *Marcal1* null mutant, *Brca2* mutant, and *Marcal1 Brca2* double mutant frequencies were all significantly reduced compared to wild type. The numbers of single males (biological replicates) and total progeny scored are listed below the graph. (B) EJ events were measured as the percentage of scored progeny with yellow eyes. *Brca2* and *Marcal1 Brca2* mutants had significantly elevated EJ compared to wild type and *Marcal1* single mutants. *P*-values: ****, P <0.0001, **,P <0.002, *, P <0.05, based on parametric ANOVA. (C) Synthesis tracts in repair events recovered in yellow-eyed progeny were measured using a series of PCRs. Each interval was measured independently and quantified as a percentage of total independent events analyzed. *X*-axis denotes distance (in nucleotides) from each end of the gap, on the same scale as the schematic of $P\{w^a\}$ below. *Y*-axis is percent of events analyzed that had a positive PCR and therefore synthesized at least as far as the most internal primer.*Marcal1* (n= 90) was not significantly different from wild type (n=48) when corrected for multiple intervals (Materials and Methods). *Blm* (n=75) mutants were significantly different (P <0.0001) from both wild type and *Marcal1*.

in *Marcal1* mutants was similar in length to those of wild-type flies but significantly longer tracts in *Blm* mutants (Figure 4C). Repeated rounds of strand exchange, synthesis, and D-loop dissociation have been observed in previous assays of gap repair (McVey *et al.* 2004b) and our finding that aggregated synthesis tract lengths in *Marcal1* mutants is similar to wild type suggests that the length of synthesis per cycle, while likely having some stochastic component, is unchanged by loss of Marcal1. Also, we did not observe any flanking deletions among EJ repair products from *Marcal1* mutants, whereas 48% of EJ repair in *Blm* mutant was associated with deletion. Altogether, these data suggest that the reduction in red-eyed progeny in *Marcal1* mutants is not due to defects in synthesis or inability to disassemble D-loops. These data support the hypothesis that *Marcal1* mutants have a defect in LTR annealing.

Marcal1 mediates annealing independent of synthesis

SMARCAL1 annealing studies have been restricted to replication-associated roles and we observed reduced annealing in *Marcal1* mutants using the $P\{w^a\}$ assay, which requires synthesis for annealing. We wanted to know if Marcal1 mediates annealing in contexts that do not require synthesis, so we used SSA assay called $P\{wIw\}$ (Rong and Golic 2003). $P\{wIw\}$ is a P element that has two *mini-white* (*mini-w*) genes in tandem (Figure 5, inset). The downstream copy (4.3 kb) is functional, while the upstream copy (3.6 kb) is non-functional due to a deletion of the promoter and first exon. The two are separated by a linker region containing an *I-Sce*I recognition site and can be differentiated by amplifying FRT sites present in the 5′ region of each copy (Figure 5, inset). *I-Sce*I is expressed in the germlines of male larvae heterozygous for an insertion of $P\{wIw\}$ on chromosome 3 and repair events are recovered in the progeny (Figure 5A). Previous studies have shown that *I-Sce*I cuts at >90% efficiency in this

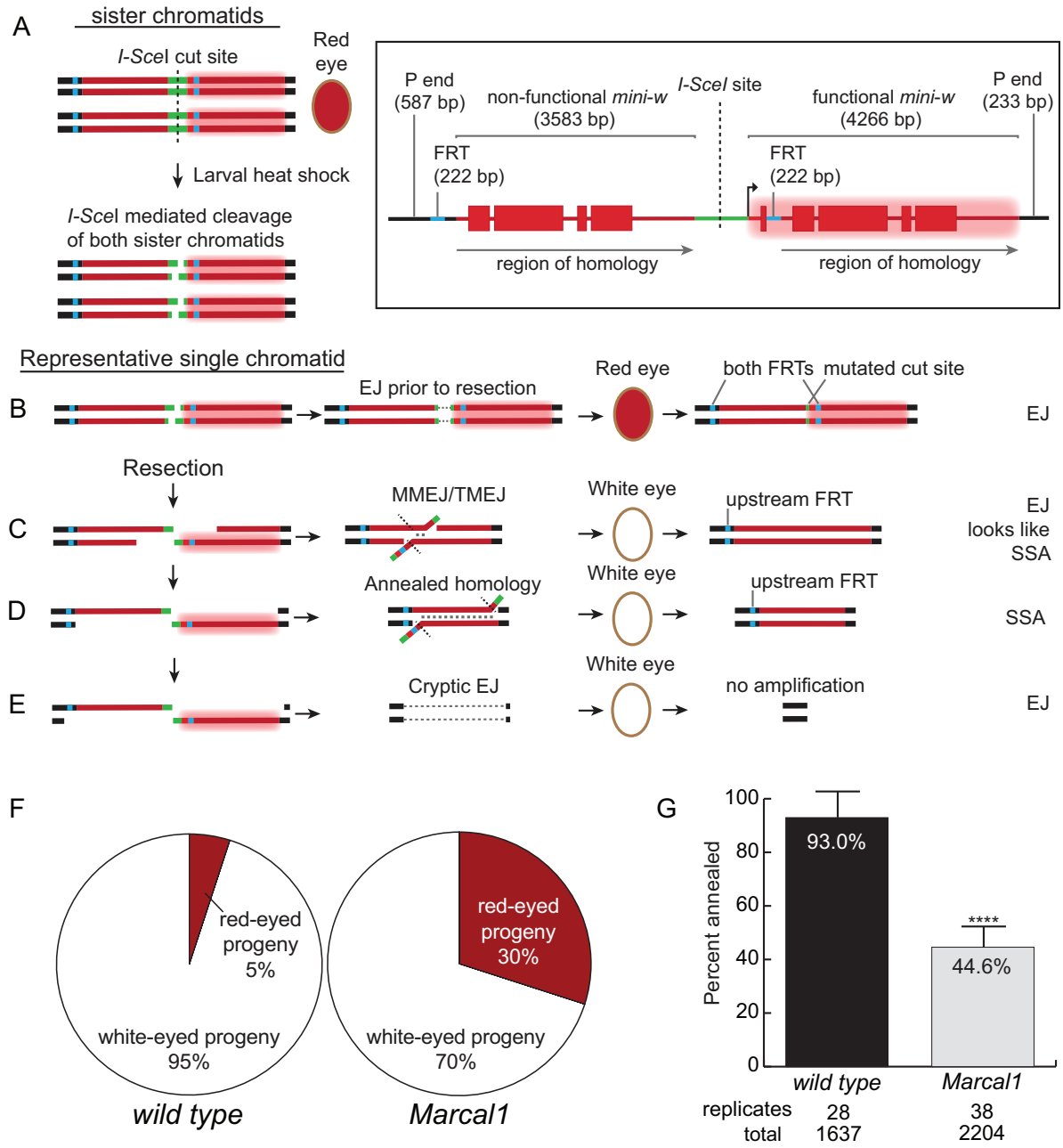

Figure 5 ***Marcal1*** **mutants have reduced annealing capacity in the** ***P{wIw}*** **assay.** *Inset*: The construct is on chromosome *3* and consists of two copies of the *mini-white* (*mini-w*) gene that are tandemly arrayed and separated by a linker containing an *I-Sce*I recognition site. The upstream copy is missing exon 1 and intron 1 rendering it non-functional, while the downstream copy is functional (represented by a red glow in the schematic), and produces a wild-type red eye in a *w* null background. The upstream *mini-w* has a 5′ FRT site and the downstream copy has an FRT insertion in intron 1. PCR amplification of the FRT anchored in *mini-w* yields different size products for each gene which is used to identify the presence or absence of each copy. (A) The assay is performed in the male germline with *P{wIw}* heterozygous. *I-Sce*I is expressed via heat shock during larval development, resulting in DSBs with 4-nt overhangs on both sister chromatids. (B) Mutational cNHEJ can occur at the cut site, yielding red-eyed progeny and the presence of both FRTs but a mutated *I-Sce*I cut site. (C) If resection is insufficient to expose complementary sequences, MMEJ/TMEJ can give white-eyed progeny with a deletion that includes the downstream FRT. These events cannot be differentiated from products of SSA unless the deletion is sufficiently large (>1000 bp); if no difference in size was observed, these events were classified as SSA. (D) Full resection of at least 3.6 kb reveals complementarity between the ssDNA ends that can be annealed. This results in white-eyed progeny with only the upstream FRT site; such events were categorized as SSA. (E) Excessive resection can result in deletion of the entire construct, resulting in white-eyed progeny with no amplification products. (F) Percentage of total progeny with white or red eyes for wild type and *Marcal1* mutants. $P < 0.0001$ using χ^2 test. (G) Percentage of repair products that involved annealing, after molecular analysis correction (Figure S2). *Marcal1* null mutants had significantly reduced annealing compared to wild type, $P < 0.0001$. Error bars are SD. Biological replicates (single males) and total progeny scored are denoted below each genotype.

context, thus the most common outcome is cutting of both sister chromatids (Rong and Golic 2003). Since the homologous chromosome does not have a *P{wIw}* insertion, strand invasion is a rare event; however, full resection of both sides can reveal the 3.6 kb of complementarity between the upstream and downstream copies of *mini-w*. If these sequences are annealed, completion of SSA repair gives a product that retains only a non-functional copy of *mini-w*; progeny that inherit this repair event will have white eyes and the upstream FRT site. Red-eyed progeny can result from EJ with little or no resection or from an uncut construct; which will have both FRT sites and a mutated *I-Sce*I cut site (Figure 5A). White eyes can also result from EJ repair with deletion into the promoter of the downstream *mini-w*, which will have both FRT sites; however, EJ events with deletions that extend into the downstream FRT site can be indistinguishable from SSA events.

We observed a significant difference in the distribution of eye color between wild type and *Marcal1* mutants (Figure 5B). Every *Marcal1* mutant male had progeny with both eye colors, whereas almost 40% of wild-type males did not produce any red-eyed progeny. We collected 10 (or all if less than 10) red-eyed progeny from each male for molecular analyses. These analyses showed no difference in cutting efficiency of *I-Sce*I between *Marcal1* and wild type (Figure S2), suggesting that the increase in red-eyed progeny in *Marcal1* mutants is not due to reduced induction of DSBs. Furthermore, the distribution of EJ events in red-eyed flies was strikingly similar between *Marcal1* and wild type, which suggests that the type of EJ utilized is not affected by Marcal1. This is consistent with a role for Marcal1 after resection since the type of EJ is dictated by the structure of the DNA ends.

We also collected 10 white-eyed progeny for analysis. 98% of the white-eyed males from wild-type flies were consistent with annealing by SSA (Figure S2). In stark contrast, 34% of analyzed white-eyed progeny from *Marcal1* mutant males were confirmed as EJ. It is likely that this number is under-reported because the large regions of homology in the construct obscures identification of EJ events that are similar in size to the predicted annealed length. Altogether, these data show significantly reduced SSA annealing capacity in *Marcal1* null mutants (44.6%) compared to wild type (93.0%) (Figure 5C), indicating Marcal1 is important for annealing in both synthesis-dependent (SDSA) and synthesis-independent (SSA) repair strategies.

ATP-binding is required for Marcal1 activity during SDSA

We next asked if Marcal1 translocation is required for annealing during SDSA. Helicases use the conserved Walker A and Walker B motifs to bind and hydrolyze ATP for translocation. SMARCAL1 can bind DNA in the absence of ATP (Yusufzai and Kadonaga 2008), so we abolished the ATP-binding site in the Walker A motif by mutating the conserved lysine to a methionine (K275M) in the endogenous *Marcal1* gene via CRISPR/Cas9. We then tested the ability of $Marcal1^{K275M}$ ATP-binding defective mutants to repair a gap using the $P\{w^a\}$ assay. $Marcal1^{K275M}$ mutants had a reduction in SDSA similar to that of *Marcal1* null mutants (Figure 6A), suggesting that translocation is required for its function during SDSA. Surprisingly, EJ events were significantly reduced compared to wild type and *Marcal1* null mutants (Figure 6B), revealing a genetic interaction between Marcal1 and EJ pathways. We compared synthesis patterns in $Marcal1^{K275M}$ mutants to wild type and *Marcal1* null mutants. We found that $Marcal1^{K275M}$ mutants did not have significantly different synthesis length compared to either genotype (Figure 6C).

Lastly, we tested the ability of $Marcal1^{K275M}$ mutants and $Marcal1^{K275M}$ heterozygotes to anneal complementary sequences during SSA using the *P{wIw}* assay. White-eyed flies were significantly decreased in $Marcal1^{K275M}$ mutants (66.88%), compared to $Marcal1^{K275M}$ heterozygotes (95.59%) (Figure 6D). The white-eyed frequency in heterozygotes was not statistically different from wild type (wild type data from Figure 5B) and like wild type, 40% of $Marcal1^{K275M}$ heterozygous males had no red-eyed progeny (all $Marcal1^{K275M}$ homozygous males had red-eyed progeny). The percentage of red- and white-eyed progeny in $Marcal1^{K275M}$ mutants was not significantly different from *Marcal1* null mutants (null data from Figure 5B), suggesting that ATP-binding does not affect EJ in the absence of strand exchange, synthesis, and D-loop dissociation. These data also show that ATP-binding is required for annealing during SSA, supporting our findings from $P\{w^a\}$ and establishing a requirement for ATP hydrolysis in annealing activities of Marcal1.

Discussion

DSB repair strategies can be thought of as a series of choices that are made by weighing a combination of complex factors, including availability of a repair template, cell cycle timing, nuclear architecture, and the chromatin context of the break itself. The first key decision point is resection, which dictates a commitment to HDR strategies (sequestering the ends of the break from resection results in direct ligation via cNHEJ (reviewed in Mimitou and Symington 2009). Brca2 acts downstream of resection to facilitate strand exchange with the template and the phenotype of *Brca2 Marcal1* double mutants shows *Brca2* is epistatic to *Marcal1*, indicating that Marcal1 acts later in the HDR pathway and is unlikely to be involved in resection.

Resection almost invariably leads to strand exchange and synthesis. SSA is an exception, but this can occur only when there are direct repeats flanking the break and perhaps primarily when there is no available template for HDR; it is unclear how much SSA is utilized outside of specialized assays such as *P{wIw}*. Regardless, SSA is efficiently used in specific situations and the data presented here provide evidence that it shares a common annealing mediator, Marcal1, with other HDR strategies.

The second key decision point in HDR repair is disassembly of the D-loop, which dictates the choice between SDSA and the dHJ pathway. Disassembly favors SDSA by promoting complementarity tests and annealing, whereas continued synthesis increases the likelihood of 2nd-end capture and dHJ formation. In *Drosophila*, Blm helicase has been identified as a key mediator of D-loop disassembly (Adams *et al.* 2003; McVey *et al.* 2004a), and recent studies suggest Fancm may play a minor role in this step as well (Kuo *et al.* 2014; Romero *et al.* 2016), though studies in human cells do not show a role for FANCM in SDSA (Zapotoczny and Sekelsky 2017). We did not observe phenotypes suggesting defects in D-loop dissociation in *Marcal1* mutants, suggesting that the role of Marcal1 is downstream of D-loop dissociation.

The third key decision point is annealing, which we propose impacts the choice between SDSA, EJ (primarily TMEJ), and re-invasion. Prior to the studies reported here, little was known about annealing during HDR in animals or how the decision between these three options is regulated. Our data here provide in vivo evidence that Marcal1 mediates annealing during SDSA and SSA in *Drosophila*, and suggest that Marcal1 acts directly to anneal complementary strands, as abrogating Marcal1

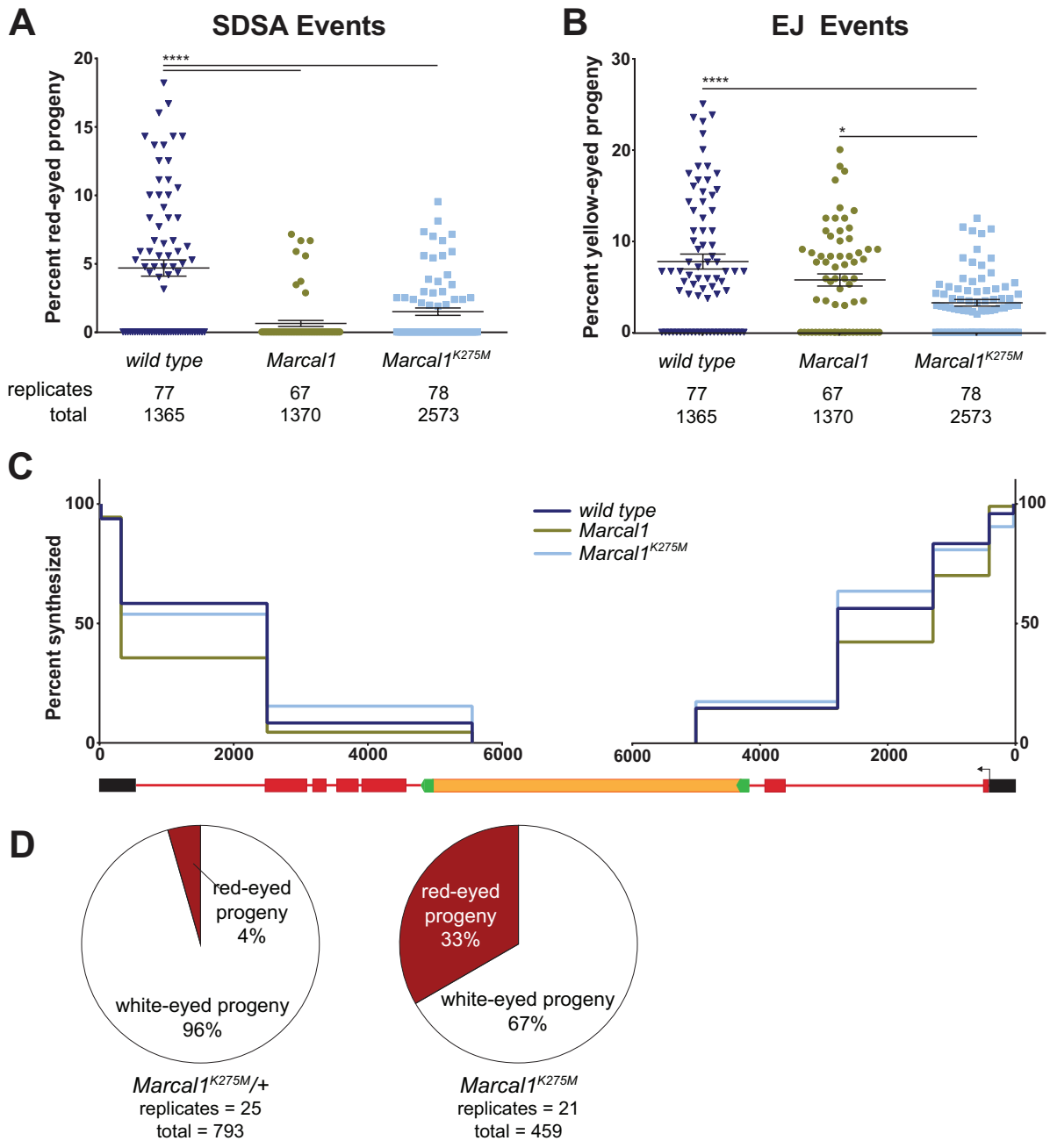

Figure 6 *Marcal1*^{K275M} mutants have reduced SDSA and EJ capacity. SDSA (A) and EJ (B) events were measured in *Marcal1*^{K275M} mutants as described in Figure 4. SDSA was similar between *Marcal1*^{K275M} and *Marcal1* null, but EJ events were significantly reduced in *Marcal1*^{K275M} compared to both wild type and *Marcal1* null mutants. (C) Synthesis tracts lengths, measured as described in Figure 4C. No significant differences were found between *Marcal1*^{K275M} (n=52) and wild type (n = 48) or *Marcal1* null mutants (n=90). (D) *Marcal1*^{K275M} heterozygotes and *Marcal1*^{K275M} mutants were tested in the *P{wIw}* SSA assay as described in Figure 5. Heterozygotes had 96% white-eyed progeny, which is not statistically different from wild type (Figure 5F) based on a parametric ANOVA test. *Marcal1*^{K275M} mutants had 67% white-eyed progeny, which was significantly reduced compared to heterozygotes but not significantly different from *Marcal1* null mutants (Figure 5F).

translocation activity via Walker A mutation recapitulates the null phenotype.

The *Marcal1*^{K275M} mutation reduces EJ as well as annealing during SDSA, which suggests that *Marcal1*^{K275M} antagonizes EJ in contexts where EJ follows strand exchange, synthesis, and D-loop dissociation. EJ in *Marcal1* null mutants is unaffected, which further suggests the EJ phenotype in *Marcal1*^{K275M} mutants is likely due to defective annealing activity leading to aberrant interactions with the DNA rather than a non-annealing protein-protein interaction. We propose the *Marcal1*^{K275M} phenotype is a consequence of localization to the DNA without translocation activity, which may indicate Marcal1 precedes recruitment of EJ factors after D-loop dissociation. Further studies are needed to test this hypothesis.

Interestingly, we observed that *Marcal1*^{K275M} is completely recessive in the *P{wIw}* assay (Figure 6D). It is possible that *Marcal1*^{K275M} mutant protein may bind DNA less tightly than the wild-type protein. While ATP-binding is not required for DNA binding by SMARCAL1, it can cause a conformational change that influences the DNA binding constant (Gupta *et al.* 2015). It is also possible that multiple Marcal1 molecules bind the nascent DNA and the presence of any wild-type protein is sufficient to rescue the *Marcal1*^{K275M} phenotype. Recent work on the RPA-SMARCAL1 interface has shown that SMARCAL1 binds to the C-terminal region of RPA32 with 1:1 stoichiometry (Bhat *et al.* 2014; Xie *et al.* 2014) and it is likely that many molecules of Marcal1 bind the RPA-coated nascent DNA, allowing for multiple complementarity searches to occur simultaneously. Studies have revealed a similar mechanism for homology searching by Rad51-coated ssDNA (Wright and Heyer 2014; Qi and Greene 2016). Mutation of the Walker B motif to allow ATP binding (thus preserving DNA binding kinetics) but prevent ATP hydrolysis (translocation) as well as in vitro studies of Marcal1 interactions with long RPA-bound filaments may help to clarify the mechanistic basis of the *Marcal1*^{K275M} phenotype.

An intriguing finding from our study is that synthesis tract length is not elevated in *Marcal1* mutants even though annealing is defective. Early studies of gap repair in *Drosophila* have shown that continuous synthesis averages 1379 bp and complete restoration decreases as template length increases (Gloor *et al.* 1991); additional studies with the *P{w^a}* assay suggest that gap filling involves multiple cycles of strand exchange, synthesis, and D-loop dissociation (McVey *et al.* 2004a). These attributes appear unaffected in *Marcal1* mutants suggesting that the choice to strand re-invade or EJ during a given round is not solely dependent on the outcome of complementarity tests even though, the reduction in EJ in *Marcal1*^{K275M} mutants argues that *Marcal1* is recruited to the nascent ends prior to recruitment of EJ factors. It is possible that rounds of strand invasion, synthesis, and D-loop disassembly are simply stochastic in nature, and after each a complementarity test is performed by Marcal1. When Marcal1 is present but defective, EJ factors may be excluded after D-loop dissociation, whereas when Marcal1 is completely absent EJ factors would have access to the DNA, but EJ would still be reliant on the synthesis machinery and unknown regulatory signals. These data support a model where complementarity tests are upstream of the EJ vs. strand re-invade decision but have no effect on that decision if annealing is unsuccessful. Further studies of genetic interactions between *Marcal1* and EJ factors may help to clarify this interaction.

Unlike *P{w^a}*, the *P{wIw}* assay did not reveal any differences between *Marcal1*^{K275M} and null mutants. *P{w^a}* requires multiple iterations of the anneal vs. EJ vs. re-invade decision (McVey *et al.* 2004a), providing increased opportunities to observe moderate defects in that decision among repair products. On the other hand, in the *P{wIw}* assay there is usually no intact homologous template for repair (in wild-type flies, <1% of the products were uncut or restored to the original sequence). While it is not possible to determine which repair strategy is initially favored at the break, the efficiency of *I-Sce*I cutting may ultimately select for HDR, since direct ligation would often restore the cut site, perhaps to be cut again. Once resected, annealing becomes the strongly favored strategy since long ssDNA tails are not ideal substrates for TMEJ or cNHEJ (Waters *et al.* 2014; Wyatt *et al.* 2016) and strand invasion is not possible. SSA represents over 93% of all repair products in wild type and *Marcal1*^{K275M} heterozygotes, supporting this interpretation. Because the anneal vs. EJ vs. strand re-invade decision point is highly altered and potentially de-regulated by the assay design, it is likely that EJ events in *P{wIw}* are facilitated through alternative pathways that are less influenced by Marcal1. Our data support this interpretation as we see a large (>7-fold) increase in EJ events in both *Marcal1*^{K275M} and null mutants. These EJ events are predominantly joined near the break site without large deletions, suggesting an alternative form of EJ is utilized on long resected ends when annealing is compromised. EJ was reported by Chan *et al.* in mutants defective in both cNHEJ and TMEJ (Chan *et al.* 2010), though the key mediator of this form of EJ remains unknown.

We observed phenotypes indicative of residual annealing activity in *Marcal1* mutants. It is possible that another protein is capable of some annealing, though *Drosophila* lacks orthologs of other candidate annealases such as Rad52 and of ZRANB3 (an annealing helicase paralog of SMARCAL1). It is more likely that our observation reveals key limitations in the ability to differentiate annealed events vs. MMEJ/TMEJ using both the *P{w^a}* and the *P{wIw}* assay. In *P{w^a}*, restoration of *w* gene function is interpreted as LTR annealing, however, it is possible that EJ near the LTR could also result in restoration of *w* and the size of insertion tolerated before *w* function is compromised remains unknown. It is possible that synthesis and MMEJ/TMEJ that occurs past the LTRs can result in red-eyed progeny. Extensive synthesis past the LTRs may result in apricot eyes that would not be recovered for analysis, which may also explain why we did not observe a compensatory increase in EJ events in *Marcal1* mutants, as well.

The limitations of *P{wIw}* are predominantly due to extensive homology to either side of the break, which makes it difficult to definitively identify annealed events vs. MMEJ/TMEJ of approximately the same size. Molecular analysis revealed that 22% of white-eyed progeny in *Marcal1* mutants had this type of event (Figure S2) and it is highly probable that the true percentage is even higher but sequence similarity is an impediment to fine-scale amplification. Amplification of the entire construct followed by single-molecule sequencing, as done in the *S. cerevisiae* gap repair assay of Guo *et al.*, might allow sampling of a larger number of repair events from multiple tissues of a single individual and it could be further adapted to recover events in different progeny from a single male germline, as in our strategy (Guo *et al.* 2015). Our work has highlighted the need for fine-scale assays capable of distinguishing true annealing events from microhomology-mediated events.

The findings reported here provide evidence that Marcal1 mediates annealing in both SDSA and SSA. We have further

shown that Marcal1 impacts EJ pathways (most likely TMEJ) during HDR, providing new information on the regulation of the anneal—EJ—strand re-invade decision point. Understanding this decision has broad implications for multiple applications including chemotherapeutics and genome editing technologies. Many cancer drugs generate DSBs as a primary mechanism; the role in DSB repair discovered here suggests SMARCAL1 is important for multiple repair mechanisms during S/G2, making it an attractive target for drug development, as has been proposed by Zhang *et al.* (Zhang *et al.* 2012). Additionally, insertion of long fragments during CRISPR/Cas9 genome editing has been proposed to occur via SDSA (Byrne *et al.* 2015); understanding the regulation of SDSA will improve the efficiency of this technology. Lastly, understanding the interplay of multiple repair strategies as well as gaining insight into which strategies are used in different contexts will enhance our understanding of both the basis of genome stability disorders and their progression.

Acknowledgements

We thank E. Buzhardt and A. Cook for preliminary *Marcal1* null $P\{w^a\}$ data acquisition. This work was supported by grants from the National Institute of General Medical Sciences (NIGMS) to JS (1R01GM061252 and 1R35GM118127). JKH was supported in part by NIGMS grants 5T32GM007092 and F31GM113550.

Literature Cited

Adams, M. D., M. McVey, and J. J. Sekelsky, 2003 *Drosophila* BLM in double-strand break repair by synthesis-dependent strand annealing. Science (New York, N.Y.) **299**: 265–267.

Andersen, S. L., H. K. Kuo, D. Savukoski, M. H. Brodsky, and J. J. Sekelsky, 2011 Three structure-selective endonucleases are essential in the absence of BLM helicase in *Drosophila*. PLoS genetics **7**: e1002315.

Andersen, S. L. and J. J. Sekelsky, 2010 Meiotic versus mitotic recombination: Two different routes for double-strand break repair. BioEssays **32**: 1058–1066.

Baradaran-Heravi, A., K. S. Cho, B. Tolhuis, M. Sanyal, O. Morozova, *et al.*, 2012a Penetrance of biallelic *SMARCAL1* mutations is associated with environmental and genetic disturbances of gene expression. Human Molecular Genetics **21**: 2572–2587.

Baradaran-Heravi, A., A. Raams, J. Lubieniecka, K. S. Cho, K. A. DeHaai, *et al.*, 2012b SMARCAL1 deficiency predisposes to non-Hodgkin lymphoma and hypersensitivity to genotoxic agents *in vivo*. American journal of medical genetics **158A**: 2204–2213.

Bassett, A. R. and J.-L. Liu, 2014 CRISPR/Cas9 and genome editing in *Drosophila*. Journal of Genetics and Genomics **41**: 7–19.

Bétous, R., A. C. Mason, R. P. Rambo, C. E. Bansbach, A. Badu-Nkansah, *et al.*, 2012 SMARCAL1 catalyzes fork regression and Holliday junction migration to maintain genome stability during DNA replication. Genes & development **26**: 151–162.

Bhargava, R., D. O. Onyango, and J. M. Stark, 2016 Regulation of single-strand annealing and its role in genome maintenance. Trends in Genetics **32**: 566–575.

Bhat, K. P., R. Betous, and D. Cortez, 2014 High-affinity DNA binding domains of Replication Protein A (RPA) direct SMARCAL1-dependent replication fork remodeling. Journal of Biological Chemistry **290**: 4110–4117.

Brough, R., D. Wei, S. Leulier, C. J. Lord, Y. S. Rong, *et al.*, 2008 Functional analysis of *Drosophila melanogaster* BRCA2 in DNA repair. DNA Repair **7**: 10–19.

Byrne, S. M., L. Ortiz, P. Mali, J. Aach, and G. M. Church, 2015 Multi-kilobase homozygous targeted gene replacement in human induced pluripotent stem cells. Nucleic Acids Research **43**: e21.

Chan, S. H., A. M. Yu, and M. McVey, 2010 Dual roles for DNA Polymerase θ in alternative end-joining repair of double-strand breaks in *Drosophila*. PLoS Genetics **6**: 1–16.

Ciccia, A., A. L. Bredemeyer, M. E. Sowa, M.-E. Terret, P. V. Jallepalli, *et al.*, 2009 The SIOD disorder protein SMARCAL1 is an RPA-interacting protein involved in replication fork restart. Genes & development **23**: 2415–2425.

Ciccia, A. and S. J. Elledge, 2010 The DNA damage response: Making it safe to play with knives. Molecular Cell **40**: 179–204.

Coleman, M. A., J. A. Eisen, and H. W. Mohrenweiser, 2000 Cloning and characterization of HARP/SMARCAL1: a prokaryotic HepA-related SNF2 helicase protein from human and mouse. Genomics **65**: 274–282.

Garcia, A., R. N. Salomon, A. Witsell, J. Liepkalns, R. B. Calder, *et al.*, 2011 Loss of the bloom syndrome helicase increases DNA ligase 4-independent genome rearrangements and tumorigenesis in aging *Drosophila*. Genome Biology **12**: R121.

Ghosal, G., J. Yuan, and J. Chen, 2011 The HARP domain dictates the annealing helicase activity of HARP/SMARCAL1. EMBO reports **12**: 574–580.

Gloor, G. B., N. a. Nassif, D. M. Johnson-schlitz, C. R. Preston, and W. R. Engels, 1991 Targeted gene replacement in *Drosophila* via P element-induced gap repair. Science (New York, N.Y.) **253**: 1110–1117.

Gratz, S. J., A. M. Cummings, J. N. Nguyen, D. C. Hamm, L. K. Donohue, *et al.*, 2013 Genome engineering of *Drosophila* with the CRISPR RNA-guided Cas9 nuclease. Genetics **194**: 1029–1035.

Guo, X., K. Lehner, K. O'Connell, J. Zhang, S. S. Dave, *et al.*, 2015 SMRT sequencing for parallel analysis of multiple targets and accurate SNP phasing. G3 (Bethesda, Md.) **5**: 2801–2808.

Gupta, M., M. Mazumder, K. Dhatchinamoorthy, M. Nongkhlaw, D. T. Haokip, *et al.*, 2015 Ligand-induced conformation changes drive ATP hydrolysis and function in SMARCAL1. FEBS Journal **282**: 3841–3859.

Hammond, E. M., S. L. Green, and A. J. Giaccia, 2003 Comparison of hypoxia-induced replication arrest with hydroxyurea and aphidicolin-induced arrest. Mutation Research - Fundamental and Molecular Mechanisms of Mutagenesis **532**: 205–213.

Ira, G., A. Malkova, G. Liberi, M. Foiani, and J. E. Haber, 2003 Srs2 and Sgs1 – Top3 suppress crossovers during double-strand break repair in yeast. Cell **115**: 401–411.

Ivanov, E. L., N. Sugawara, J. Fishman-Lobell, and J. E. Haber, 1996 Genetic requirements for the single-strand annealing pathway of double-strand break repair in *Saccharomyces cerevisiae*. Genetics **142**: 693–704.

Jasin, M. and R. Rothstein, 2013 Repair of strand breaks by homologous recombination. Cold Spring Harbor perspectives in biology **5**.

Jensen, R. B., 2013 BRCA2: One small step for DNA repair, one giant protein purified. Yale Journal of Biology and Medicine **86**: 479–489.

Jensen, R. B., A. Carreira, and S. C. Kowalczykowski, 2010 Purified human BRCA2 stimulates RAD51-mediated recombina-

tion. Nature **467**: 678–683.

Kassavetis, G. a. and J. T. Kadonaga, 2014 The annealing helicase and branch migration activities of Drosophila HARP. PloS one **9**: e98173.

Khade, N. V. and T. Sugiyama, 2016 Roles of C-terminal region of yeast and human rad52 in rad51-nucleoprotein filament formation and ssDNA annealing. PLoS ONE **11**: 1–14.

Kuo, H. K., S. McMahan, C. M. Rota, K. P. Kohl, and J. Sekelsky, 2014 *Drosophila* FANCM helicase prevents spontaneous mitotic crossovers generated by the MUS81 and SLX1 nucleases. Genetics **198**: 935–945.

Kurkulos, M., J. M. Weinberg, D. Roy, and S. M. Mount, 1994 P element-mediated *in vivo* deletion analysis of *white-apricot*: Deletions between direct repeats are strongly favored. Genetics **136**: 1001–1011.

LaFave, M. C., S. L. Andersen, E. P. Stoffregen, J. K. Holsclaw, K. P. Kohl, *et al.*, 2014 Sources and structures of mitotic crossovers that arise when BLM helicase is absent in *Drosophila*. Genetics **196**: 107–118.

LaRocque, J. R., B. Jaklevic, T. S. Tin, and J. Sekelsky, 2007 *Drosophila* ATR in double-strand break repair. Genetics **175**: 1023–1033.

Lou, S., P. Lamfers, N. McGuire, and C. F. Boerkoel, 2002 Longevity in Schimke immuno-osseous dysplasia. Journal of medical genetics **39**: 922–925.

Lundin, C., M. North, K. Erixon, K. Walters, D. Jenssen, *et al.*, 2005 Methyl methanesulfonate (MMS) produces heat-labile DNA damage but no detectable *in vivo* DNA double-strand breaks. Nucleic acids research **33**: 3799–3811.

Maede, Y., H. Shimizu, T. Fukushima, T. Kogame, T. Nakamura, *et al.*, 2014 Differential and common DNA repair pathways for topoisomerase I- and II-targeted drugs in a genetic DT40 repair cell screen panel. Molecular cancer therapeutics **13**: 214–220.

McIlwraith, M. J. and S. C. West, 2008 DNA repair synthesis facilitates RAD52-Mediated second-end capture during DSB repair. Molecular Cell **29**: 510–516.

McVey, M., M. Adams, E. Staeva-Vieira, and J. J. Sekelsky, 2004a Evidence for multiple cycles of strand invasion during repair of double-strand gaps in *Drosophila*. Genetics **167**: 699–705.

McVey, M., S. L. Andersen, Y. Broze, and J. Sekelsky, 2007 Multiple functions of *Drosophila* BLM helicase in maintenance of genome stability. Genetics **176**: 1979–1992.

McVey, M., J. R. Larocque, M. D. Adams, and J. J. Sekelsky, 2004b Formation of deletions during double-strand break repair in *Drosophila DmBlm* mutants occurs after strand invasion. Proceedings of the National Academy of Sciences of the United States of America **101**: 15694–15699.

Mimitou, E. P. and L. S. Symington, 2009 DNA end resection: Many nucleases make light work. DNA Repair **8**: 983–995.

Morimoto, M., A. Baradaran-Heravi, T. Lucke, and C. F. Boerkoel, 2016 *Schimke Immunoosseous Dysplasia*. University of Washington, Seattle, Seattle, WA.

Mukherjee, S., M. C. LaFave, and J. Sekelsky, 2009 DNA damage responses in *Drosophila nbs* mutants with reduced or altered NBS function. DNA Repair **8**: 803–812.

Nassif, N. and W. Engels, 1993 DNA homology requirements for mitotic gap repair in *Drosophila*. Proceedings of the National Academy of Sciences of the United States of America **90**: 1262–1266.

Nimonkar, A. V., R. A. Sica, and S. C. Kowalczykowski, 2009 Rad52 promotes second-end DNA capture in double-stranded break repair to form complement-stabilized joint molecules. Proceedings of the National Academy of Sciences of the United States of America **106**: 3077–3082.

Pâques, F., W. Y. Leung, and J. E. Haber, 1998 Expansions and contractions in a tandem repeat induced by double-strand break repair. Molecular and cellular biology **18**: 2045–2054.

Pfeiffer, P., W. Goedecke, and G. Obe, 2000 Mechanisms of DNA double-strand break repair and their potential to induce chromosomal aberrations. Mutagenesis **15**: 289–302.

Pommier, Y., E. Leo, H. Zhang, and C. Marchand, 2010 DNA topoisomerases and their poisoning by anticancer and antibacterial drugs. Chemistry and Biology **17**: 421–433.

Povirk, L. F. and D. E. Shuker, 1994 DNA damage and mutagenesis induced by nitrogen mustards. Mutation Research/Reviews in Genetic Toxicology **318**: 205–226.

Qi, Z. and E. C. Greene, 2016 Visualizing recombination intermediates with single-stranded DNA curtains. Methods **105**: 62–74.

Radford, I. R., 1985 The level of induced DNA double-strand breakage correlates with cell killing after x-irradiation. International Journal of Radiation Biology **48**: 45–54.

Reuter, M., A. Zelensky, I. Smal, E. Meijering, W. A. van Cappellen, *et al.*, 2014 BRCA2 diffuses as oligomeric clusters with RAD51 and changes mobility after DNA damage in live cells. Journal of Cell Biology **207**: 599–613.

Rijkers, T., J. Van Den Ouweland, B. Morolli, A. G. Rolink, W. M. Baarends, *et al.*, 1998 Targeted inactivation of mouse *RAD52* reduces homologous recombination but not resistance to ionizing radiation. Molecular and Cellular Biology **18**: 6423–6429.

Rodgers, K. and M. McVey, 2016 Error-prone repair of DNA double-strand breaks. Journal of Cellular Physiology **231**: 15–24.

Romero, N. E., S. W. Matson, and J. Sekelsky, 2016 Biochemical activities and genetic functions of the *Drosophila melanogaster* fancm helicase in DNA repair. Genetics **204**: 531–541.

Rong, Y. S. and K. G. Golic, 2003 The homologous chromosome is an effective template for the repair of mitotic DNA double-strand breaks in *Drosophila*. Genetics **165**: 1831–1842.

Sage, E. and N. Shikazono, 2016 Radiation-induced clustered DNA lesions: repair and mutagenesis. Free Radical Biology and Medicine p. [epub ahead of print].

Sarbajna, S., D. Davies, and S. C. West, 2014 Roles of SLX1-SLX4, MUS81-EME1, and GEN1 in avoiding genome instability and mitotic catastrophe. Genes and Development **28**: 1124–1136.

Storici, F., J. R. Snipe, G. K. Chan, D. A. Gordenin, and M. A. Resnick, 2006 Conservative repair of a chromosomal double-strand break by single-strand DNA through two steps of annealing. Molecular and cellular biology **26**: 7645–7657.

Symington, L. S. and J. Gautier, 2011 Double-strand break end resection and repair pathway choice. Annual Review of Genetics **45**: 247–271.

Thomas, A. M., C. Hui, A. South, and M. McVey, 2013 Common variants of *Drosophila melanogaster* Cyp6d2 cause camptothecin sensitivity and synergize with loss of Brca2. G3 (Bethesda, Md.) **3**: 91–99.

Tsai, A. G. and M. R. Lieber, 2010 Mechanisms of chromosomal rearrangement in the human genome. BMC genomics **11 Suppl 1**: S1.

van Schendel, R., J. van Heteren, R. Welten, and M. Tijsterman, 2016 Genomic scars generated by Polymerase θ reveal the versatile mechanism of alternative end-joining. PLOS Genetics **12**: e1006368.

Waters, C. A., N. T. Strande, D. W. Wyatt, J. M. Pryor, and D. A. Ramsden, 2014 Nonhomologous end joining: A good solution for bad ends. DNA Repair **17**: 39–51.

Williams, G. J., M. Hammel, S. K. Radhakrishnan, D. Ramsden, S. P. Lees-Miller, *et al.*, 2014 Structural insights into NHEJ: Building up an integrated picture of the dynamic DSB repair super complex, one component and interaction at a time. DNA Repair **17**: 110–120.

Wright, W. D. and W. D. Heyer, 2014 Rad54 functions as a heteroduplex DNA pump modulated by its DNA substrates and Rad51 during D-Loop formation. Molecular Cell **53**: 420–432.

Wyatt, D. W., W. Feng, M. P. Conlin, M. J. Yousefzadeh, S. A. Roberts, *et al.*, 2016 Essential roles for Polymerase θ-mediated end joining in the repair of chromosome breaks. Molecular Cell **63**: 662–673.

Xie, S., Y. Lu, J. Jakoncic, H. Sun, J. Xia, *et al.*, 2014 Structure of RPA32 bound to the N-terminus of SMARCAL1 redefines the binding interface between RPA32 and its interacting proteins. FEBS Journal **281**: 3382–3396.

Yousefzadeh, M. J., D. W. Wyatt, K. i. Takata, Y. Mu, S. C. Hensley, *et al.*, 2014 Mechanism of Suppression of Chromosomal Instability by DNA Polymerase POLQ. PLoS Genetics **10**: e1004654.

Yu, A. M. and M. McVey, 2010 Synthesis-dependent microhomology-mediated end joining accounts for multiple types of repair junctions. Nucleic Acids Research **38**: 5706–5717.

Yuan, J., G. Ghosal, and J. Chen, 2012 The HARP-like domain-containing protein AH2/ZRANB3 binds to PCNA and participates in cellular response to replication stress. Molecular Cell **47**: 410–421.

Yusufzai, T. and J. T. Kadonaga, 2008 HARP is an ATP-driven annealing helicase. Science (New York, N.Y.) **322**: 748–750.

Zapotoczny, G. and J. Sekelsky, 2017 Human cell assays for synthesis-dependent strand annealing and crossing over during double-strand break repair. G3: Genes, Genomes, Genetics **X**: 1–10.

Zhang, L., S. Fan, H. Liu, and C. Huang, 2012 Targeting SMARCAL1 as a novel strategy for cancer therapy. Biochemical and biophysical research communications **427**: 232–235.

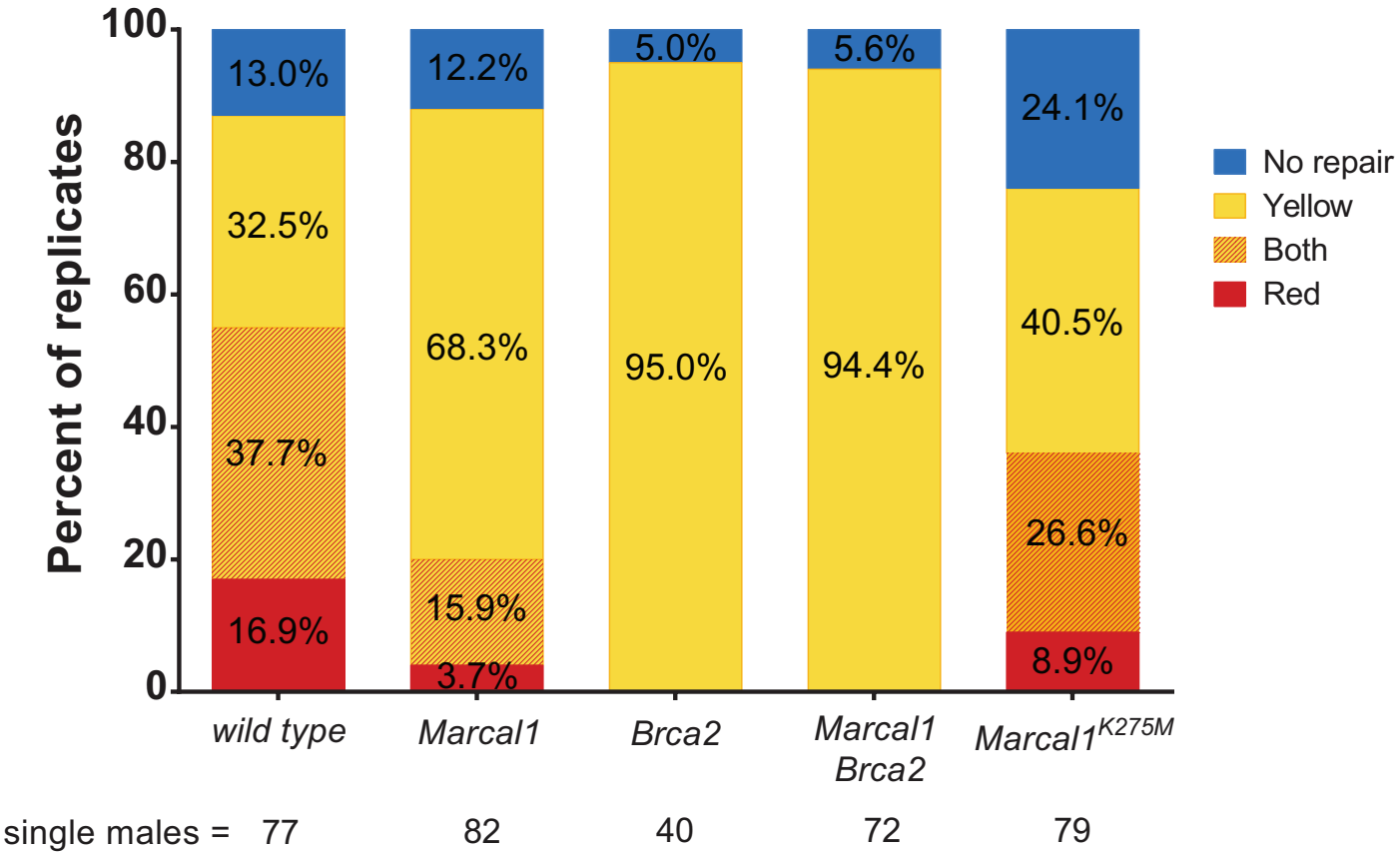

Figure S1 Distribution of repair events per replicate (single male). Each male (replicate) from the $P\{w^a\}$ assay was categorized according to the distribution of repair events observed in his progeny and the data are displayed as a percentage of all males assayed in each genotype. Red indicates red-eyed progeny were observed; yellow indicates yellow-eyed progeny; both indicates red- and yellow-eyed progeny; and no repair indicates no red or yellow-eyed progeny were observed. Apricot-eyed progeny were observed in the progeny of every male.

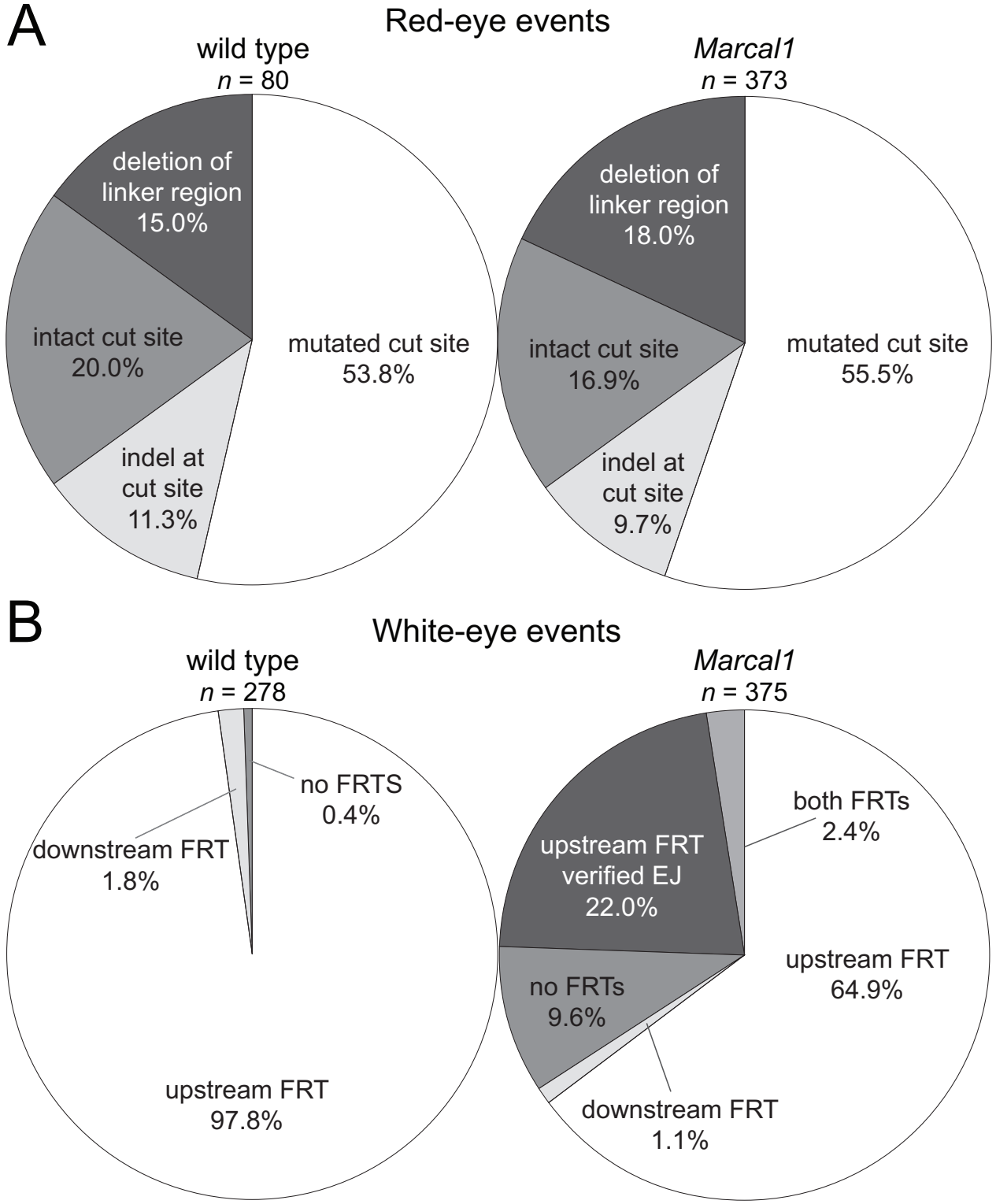

Figure S2 Distribution of *P{wIw}* events in wild type and *Marcal1* mutants after molecular analysis. A) Distribution of molecularly analyzed events from collected red-eyed progeny as a percentage of total red analyzed events (listed below genotype). Mutated cut site: amplified band (primer set wIw_cut, Table S3) was not cut with *I-Sce*I; indel at cut site: band was smaller or larger than predicted; intact cut site: band was cut with *I-Sce*I; deletion of linker region: no amplification with primer set. B) Distribution of molecularly analyzed events from collected white-eyed progeny as a percentage of total white analyzed events (listed below genotype). Upstream FRT: only FRT associated with upstream *mini-w* amplified (primer set, Table S3) (categorized as annealed events); upstream FRT verified EJ: larger or smaller than predicted products from whole construct amplification (categorized as EJ events); downstream FRT: only downstream FRT amplified (verified to be in the upstream locus, removed from final data set); both FRTs: both amplified (categorized as EJ events); no FRTs: no amplification (categorized as EJ events).

Mutagen	Dosage	Biological replicates	Unexposed progeny	Exposed progeny
Methyl methanesulfonate	3.23 mM	16	2864	1397
Nitrogen mustard	0.2 mM	22	3828	3131
Hydroxyurea	100 mM	22	3964	1841
Etoposide	10 mM	9	1098	876
Camptothecin	0.05 mM	26	3432	2233
Ionizing radiation	2000 rads (20 Gy)	19	2196	1395

Table S1 Dosage and sample sizes of mutagen exposure experiment. *Marcal1* null mutants were treated with each mutagen in separate experiments as described in Materials and Methods. Biological replicates refers to individual vials assayed, each containing a single male (ratios of wt:mutant survival were calculated per vial). Progeny counts are the aggregated total number of flies scored for each mutagen.

Description	Primer 1	Primer 2
5 bp right side	CCGCGGCCGCGGACCACCTTATGTTATTT	GCCTTGCTTCTTCCACACAGCGTG
0.9 kb right side	CCCTCGCAGCGTACTATTGAT	AGATGGGTGTTTGCTGCCTCCG
2.4 kb right side	GAGCGAGATGGCCATATGGCTG	CGTTGTTTGCACGTCTCGCTCG
4.6 kb right side (into *copia*	GGACTGGGCCCATAACCTGTTG	GAGCGACACATACCGGCG
5 bp left side	CCGCGGCCGCGGACCACCTTATGTTATTT	ACCATTGCAAGCTACATAGCTGAC
2 kb left side	GACTGTGCGTTAGGTCCTGT	CGTTTCGTAGTTGCTCTTTCGC
5.2 kb left side (all *w* exons into *copia*)	TGCCAGAGAGCAAGTTCAGA	GAGGTCATCCTGCTGGACAT

Table S2 *P*{*w*^{a}} primers. Diagram above table depicts PCR products. Sizes represent synthesis from break end, not PCR product size. The null *white* (*w*) gene in the *ywP*{*w*^{a}} genotype is a partial deletion of the 5′ end of *w* leaving the 3′ end intact. The left side of the construct above is identical to the 3′ end of *w*; therefore, all PCRs of the left end must be anchored in the *P* element ends or in *copia* to prevent amplification of the background copy of *w*.

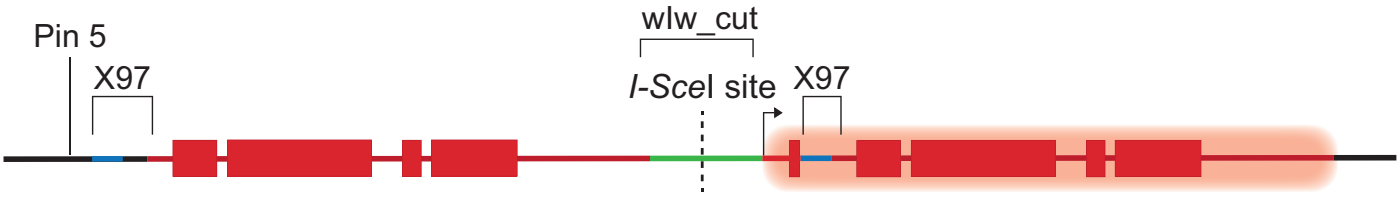

Description	Primer 1	Primer 2
X97	CGACGTGAACAGTGAGCTGT	GCTCATCTAACCCCGAACAA
wIw_cut	TGTGTGTTTGGCCGAAGTAT	CGCGATGTGTTCACTTTGCT
Pin 5	GACTGTGCGTTAGGTCCTGT	

Table S3 *P{wIw}* primers. Diagram above table depicts PCR products. The wIw_cut primer set was used to amplify the *I-Sce*I cut site in red-eyed repair events. The X97 primer set was used to assess annealing via SSA in white-eyed repair events. The upstream product is 480 bp whereas the downstream product is 369 bp. Presence of only the upstream product represents correct annealing via SSA; presence of both indicates EJ that abolishes *mini-white* function; the presence of only the downstream product was rare and verified to be in the upstream location using the Pin 5 and X97 primer 2 set. These events are interpreted as SSA with small deletions in the X97 region. Lack of amplification with the X97 primer set indicates EJ.